TMPRSS2 and furin are both essential for proteolytic activation and spread of SARS-CoV-2 in human airway epithelial cells and provide promising drug targets

Dorothea Bestle[1#], Miriam Ruth Heindl[1#], Hannah Limburg[1#], Thuy Van Lam van[2], Oliver Pilgram[2], Hong Moulton[3], David A. Stein[3], Kornelia Hardes[2,4], Markus Eickmann[1,5], Olga Dolnik[1,5], Cornelius Rohde[1,5], Stephan Becker[1,5], Hans-Dieter Klenk[1], Wolfgang Garten[1], Torsten Steinmetzer[2], and Eva Böttcher-Friebertshäuser[1*]

1) Institute of Virology, Philipps-University, Marburg, Germany

2) Institute of Pharmaceutical Chemistry, Philipps-University, Marburg, Germany

3) Department of Biomedical Sciences, Carlson College of Veterinary Medicine, Oregon State University, Corvallis, USA

4) Fraunhofer Institute for Molecular Biology and Applied Ecology, Gießen, Germany

5) German Center for Infection Research (DZIF), Marburg-Gießen-Langen Site, Emerging Infections Unit, Philipps-University, Marburg, Germany

#These authors contributed equally to this work.

*Corresponding author: Eva Böttcher-Friebertshäuser

Institute of Virology, Philipps-University Marburg

Hans-Meerwein-Straße 2, 35043 Marburg, Germany

Tel: 0049-6421-2866019

E-mail: friebertshaeuser@staff.uni-marburg.de

Short title: TMPRSS2 and furin activate SARS-CoV-2 spike protein

Abstract (295)

In December 2019, a novel coronavirus named SARS-CoV-2 first reported in Wuhan, China, emerged and rapidly spread to numerous other countries globally, causing the current pandemic. SARS-CoV-2 causes acute infection of the respiratory tract (COVID-19) that can result in severe disease and lethality. Currently, there is no approved antiviral drug for treating COVID-19 patients and there is an urgent need for specific antiviral therapies and vaccines.

In order for SARS-CoV-2 to enter cells, its surface glycoprotein spike (S) must be cleaved at two different sites by host cell proteases, which therefore represent potential drug targets. In the present study we investigated which host cell proteases activate the SARS-CoV-2 S protein in Calu-3 human airway epithelial cells. We show that S can be cleaved by both the proprotein convertase furin at the S1/S2 site and the transmembrane serine protease 2 (TMPRSS2) at the S2' site. We demonstrate that TMPRSS2 is essential for activation of SARS-CoV-2 S in Calu-3 cells through antisense-mediated knockdown of TMPRSS2 expression. Further, we show that SARS-CoV-2 replication can be efficiently inhibited by two synthetic inhibitors of TMPRSS2 and also by the broad range serine protease inhibitor aprotinin. Additionally, SARS-CoV-2 replication was also strongly inhibited by the synthetic furin inhibitor MI-1851. Combining various TMPRSS2 inhibitors with MI-1851 produced more potent antiviral activity against SARS-CoV-2 than an equimolar amount of any single serine protease inhibitor. In contrast, inhibition of endosomal cathepsins by E64d did not affect virus replication.

Our data demonstrate that both TMPRSS2 and furin are essential for SARS-CoV-2 activation in human airway cells and are promising drug targets for the treatment of COVID-19 either by targeting one of these proteases alone or by a combination of furin and TMPRSS2 inhibitors. Therefore, this approach has a high therapeutic potential for treatment of COVID-19.

Introduction

In December 2019, a new coronavirus (CoV) emerged which rapidly spreads around the world causing a pandemic never observed before with these viruses. The virus was identified as a new member of the lineage b of the genus *Betacoronavirus* that also contains the 2002 severe acute respiratory syndrome (SARS)-CoV and was named SARS-CoV-2 by the WHO. The respiratory disease caused by the virus was designated as coronavirus disease 2019 (COVID-19).

CoVs are a large family of enveloped, single-stranded positive-sense RNA viruses belonging to the order *Nidovirales* and infect a broad range of mammalian and avian species, causing respiratory or enteric diseases. CoVs have a major surface protein, the spike (S) protein, which initiates infection by receptor binding and fusion of the viral lipid envelope with cellular membranes. Like fusion proteins of many other viruses, the S protein is activated by cellular proteases. Activation of CoV S is a complex process that requires proteolytic cleavage of S at two distinct sites, S1/S2 and S2' (Fig. 1), generating the subunits S1 and S2 that remain non-covalently linked (Belouzard et al. 2009; Follis et al. 2006; Bosch et al., 2008). The S1 subunit contains the receptor binding domain, while the S2 subunit is membrane-anchored and harbours the fusion machinery. Cleavage at the S2′ site, located immediately upstream of the hydrophobic fusion peptide, has been proposed to trigger the membrane fusion activity of S (Madu et al., 2009; Walls et al., 2016). In contrast, the relevance of S cleavage at the S1/S2 site is yet not fully understood. Processing of CoV S is believed to occur sequentially, with cleavage at the S1/S2 site occurring first and subsequent cleavage at S2′. Cleavage at the S1/S2 site may be crucial for conformational changes required for receptor binding and/or subsequent exposure of the S2' site to host proteases at the stage of entry (reviewed in Head-Sargent and Gallagher, 2012; Millet and Whittaker, 2015; Hoffmann et al., 2018).

Many proteases have been found to activate CoVs *in vitro* including furin, cathepsin L, and trypsin-like serine proteases such as the transmembrane serine protease 2 (TMPRSS2), TMPRSS11A, and TMPRSS11D (reviewed in Head-Sargent and Gallagher, 2012; Millet and Whittaker, 2015; Hoffmann et al., 2018). Among them, TMPRSS2 and furin play major roles in proteolytic activation of a broad range of viruses (reviewed in Klenk and Garten, 1994; Garten, 2018; Böttcher-Friebertshäuser, 2018). TMPRSS2 is a type II transmembrane serine protease (TTSP) that is widely expressed in epithelial cells of the respiratory, gastrointestinal and urogenital tract (reviewed in Bugge et al., 2009; Böttcher-Friebertshäuser, 2018). The physiological role of TMPRSS2 is yet unknown, but TMPRSS2-deficient mice lack a discernible phenotype suggesting functional redundancy (Kim et al., 2006). In 2006, we first identified TMPRSS2 as a virus activating protease, by demonstrating that it cleaves the

surface glycoprotein hemagglutinin (HA) of human influenza A viruses (Böttcher et al., 2006). Subsequently, TMPRSS2 was shown to activate the fusion proteins of a number of other respiratory viruses including human metapneumovirus, human parainfluenza viruses as well as CoVs including SARS-CoV and Middle East respiratory syndrome (MERS)-CoV in vitro (reviewed in Böttcher-Friebertshäuser, 2018; Hoffmann et al., 2018). TMPRSS2 cleaves at single arginine or lysine residues (R/K↓), and hence, activates viral fusion proteins at so called monobasic cleavage sites. More recent studies by us and others demonstrated that TMPRSS2-deficient mice do not suffer from pathology when infected with certain influenza A virus strains, SARS-CoV and MERS-CoV, respectively, due to inhibition of proteolytic actviation of progeny virus and consequently inhibition of virus spread along the respiratory tract (Hatesuer et al., 2013; Tarnow et al., 2014; Sakai et al., 2014; Iwata-Yoshikawa et al., 2019). These studies identified TMPRSS2 as an essential host cell factor for these respiratory viruses and further demonstrated that inhibition of virus activating host cell proteases, particularly TMPRSS2, provides a promising approach for the development of therapeutics to treat respiratory virus infections. The proprotein convertase (PC) furin is a type I transmembrane protein that is ubiquitously expressed in eukaryotic tissues and cells. Furin cleaves the precursors of a broad range of proteins including hormones, growth factors, cell surface receptors and adhesion molecules during their transport along the secretory pathway at multibasic motifs of the preferred consensus sequence R-X-R/K-R↓ (reviewed in Garten, 2018). Moreover, furin has been identified as an activating protease for the fusion proteins of a broad range of viruses including highly pathogenic avian influenza A viruses (HPAIV), human immunodeficiency virus (HIV), Ebola virus, Measles virus, and Yellow Fever virus as well as bacterial toxins such as Shiga toxin or anthrax toxin at multibasic motifs (reviewed in Klenk and Garten, 1994; Rockwell et al., 2002; Garten, 2018). Acquisition of a multibasic cleavage site by insertion of basic amino acids has long been known to be a prime determinant of avian influenza A virus pathogenicity in poultry. Activation of the surface glycoprotein HA of HPAIV by furin supports systemic spread of infection with often lethal outcome. In contrast, the HA of low pathogenic avian influenza A viruses (LPAIV) is activated at a monobasic cleavage site by trypsin-like serine proteases. Appropriate proteases are believed to be expressed in the respiratory and intestinal tract of birds, confining spread of infection to these tissues.

A recent study by Hoffmann et al. indicates that TMPRSS2 is also involved in SARS-CoV-2 S protein activation (Hoffmann et al., 2020). The authors show that transient expression of TMPRSS2 in Vero cells supports cathepsin-independent entry of SARS-CoV-2 pseudotypes. Moreover, pretreatment of human Caco-2 colon and human airway cells with the broad range inhibitor camostat mesylate that also inhibits TMPRSS2 activity, markedly reduced entry of SARS-CoV-2 as well as VSV pseudotypes containing the SARS-CoV-2 S protein. This

indicates that a trypsin-like serine protease is crucial for SARS-CoV-2 entry into these cells. However, sequence analysis of the SARS-CoV-2 S protein suggests that furin may also be involved in S processing (Fig. 1B; Coutard et al., 2020; Walls et al., 2020). The S1/S2 site of SARS-CoV-2 S protein contains an insertion of four amino acids providing a minimal furin cleavage site (R-R-A-R_{685}↓) in contrast to the S protein of SARS-CoV. Instead, similar to SARS-CoV the S2' cleavage site of SARS-CoV-2 S possesses a paired dibasic motif with a single KR segment (KR_{815}↓) that is recognized by trypsin-like serine proteases.

In the present study we demonstrate that the S protein of SARS-CoV-2 is activated by TMPRSS2 and furin. We also show that inhibitors against both proteases strongly suppress virus replication in human airway epithelial cells and that the combination of both types of inhibitors has a synergistic effect on virus reduction. Our results show that this approach has a high therapeutic potential for treatment of COVID-19.

Results

Cleavage of SARS-CoV-2 S1/S2 site FRET-substrates by furin

The S1/S2 cleavage site of the novel emerged SARS-CoV-2 has been shown to possess a minimal furin consensus motif of the sequence R-R-A-R↓ with an alanine instead of a basic residue in P2 position (Fig. 1B; Coutard et al., 2020; Walls et al., 2020). Only few furin substrates possess a nonbasic residue in P2 position, such as *Pseudomonas aeruginosa* exotoxin A or Shiga toxin (Rockwell et al., 2002; Garten, 2018). To test, whether the S1/S2 sequence of SARS-CoV-2 S protein is efficiently cleaved by furin, a small series of Fluorescence Resonance Energy Transfer (FRET) substrates was synthesized (Fig. 2A). All compounds possess a 3-nitrotyrosine amide as P4' residue and a 2-amino-benzoyl fluorophore in P7 position. The analogous sequences of the S proteins from MERS-CoV, SARS-CoV, and avian infectious bronchitis virus (IBV) strain Beaudette were prepared as reference substrates. Moreover, two FRET substrates of the SARS-CoV-2 S1/S2 cleavage site with P2 A→K and A→R mutations were synthesized, to evaluate whether they could constitute even more efficient cleavage sites for furin than the wild-type. The FRET substrates were tested in an enzyme kinetic assay with human furin, and their cleavage efficiency is shown in Figure 2B. The FRET substrate of the SARS-CoV-2 S1/S2 cleavage site was efficiently cleaved by recombinant furin. In contrast, the monobasic SARS-CoV FRET substrate was not processed by furin. The MERS-CoV S1/S2 FRET substrate possessing a dibasic R-X-X-R motif was cleaved by furin approximately 10-fold less efficiently than the best substrates of this FRET series. The FRET substrate SARS-CoV-

2_M1, which contains an optimized furin recognition site by virtue of an A→K mutation in P2 position, was cleaved with similar efficiency compared to the wild-type sequence. However, substitution of A→R in the P2 position strongly enhanced cleavage by furin. As expected, the analogous reference sequence of IBV was also processed by furin very efficiently. The data show that the R-R-A-R motif at the S1/S2 cleavage site of SARS-CoV-2 S is efficiently cleaved by furin *in vitro*.

SARS-Cov-2 spike protein is cleaved by both furin and TMPRSS2

We next examined whether the SARS-CoV-2 S protein is cleaved by endogenous furin in HEK293 cells. Cells were transiently transfected with pCAGGS plasmid encoding the SARS-CoV-2 S protein with a C-terminal Myc-6xHis-tag, and incubated in the absence and presence of the potent synthetic furin inhibitor MI-1851 (cf. Fig. S1; manuscript in preparation). At 24 h post transfection, cell lysates were subjected to SDS-PAGE and Western blot analysis using antibodies against the Myc epitope. As shown in Fig. 2C, the uncleaved precursor S and the S2 subunit were detected in the absence of MI-1851, indicating that S is cleaved by endogenous proteases at the S1/S2 site in HEK293 cells. S cleavage was efficiently prevented by MI-1851. In contrast, S cleavage was not prevented by the trypsin-like serine protease inhibitor aprotinin. Thus, the data indicate that SARS-CoV-2 S protein is cleaved by furin at the S1/S2 site in HEK293 cells.

We then investigated SARS-CoV-2 S cleavage by TMPRSS2. Since HEK293 cells do not express endogenous TMPRSS2 (unpublished data; see also www.proteinatlas.org), we co-transfected the cells with pCAGGS-S-Myc-6xHis and pCAGGS-TMPRSS2. Then, the cells were incubated in the absence or presence of MI-1851 to suppress S cleavage by endogenous furin. Interestingly, two S cleavage products of approximately 95 and 80 kDa, respectively, were detected upon co-expression of TMPRSS2 in the absence of MI-1851 (Fig. 2C), most likely S2 and S2‘, as they can both be detected by the Myc-specific antibody (cf. Fig. 1A). In the presence of MI-1851, only a minor S2 protein band was detected. However, the amount of S2‘ protein present in transient TMPRSS2 expressing cells was similar in MI-1851 treated and untreated cells, suggesting that S cleavage at the S2‘ site is only caused by TMPRSS2 activity. The small amount of S2 protein detected in TMPRSS2-expressing cells in the presence of MI-1851 was likely due to residual furin activity rather than cleavage of S at the S1/S2 site by TMPRSS2. Together, the data show that SARS-CoV-2 can be cleaved by furin and by TMPRSS2. The data further suggest that the proteases cleave S at different sites with furin processing the S1/S2 site and TMPRSS2 cleaving at the S2‘ site.

Knockdown of TMPRSS2 prevents proteolytic activation and multiplication of SARS-CoV-2 in Calu-3 human airway epithelial cells

Next, we wished to investigate whether TMPRSS2 is involved in proteolytic activation and multicycle replication of SARS-CoV-2 in Calu-3 human airway epithelial cells. To specifically knockdown TMPRSS2 activity, we previously developed an antisense peptide-conjugated phosphorodiamidate morpholino oligomer (PPMO) (Böttcher-Friebertshäuser et al., 2011). PPMO are single-stranded nucleic acid-like compounds, composed of a morpholino oligomer covalently conjugated to a cell-penetrating peptide, and can interfere with gene expression by sterically blocking complementary RNAs. PPMO are water-soluble and achieve entry into cells and tissues without assisted delivery (reviewed in Stein, 2008; Moulton and Moulton, 2010). The previously developed PPMO T-ex5 interferes with correct splicing of TMPRSS2 pre-mRNA, resulting in the production of mature mRNA lacking exon 5 and consequently expression of a truncated TMPRSS2 form that is enzymatically inactive. Using T-ex5 PPMO-mediated knockdown of TMPRSS2 activity, we were able to identify TMPRSS2 as the major influenza A virus activating protease in Calu-3 cells and primary human airway epithelial cells and of influenza B virus in primary human type II pneumocytes (Böttcher-Friebertshäuser et al., 2011; Limburg et al., 2019).

Here, Calu-3 cells were treated once with T-ex5 PPMO for 24 h prior to infection with SARS-CoV-2 in order to inhibit the production of normal TMPRSS2-mRNA and deplete enzymatically active TMPRSS2 present in the cells. The cells were then inoculated with SARS-CoV-2 at a low multiplicity of infection (MOI) of 0.001, further incubated without additional PPMO treatment for 72 h, then fixed and immunostained using an antiserum against the 2002 SARS-CoV. As shown in Fig. 3A, a strong cytopathic effect (CPE) and efficient spread of SARS-CoV-2 infection was visible in Calu-3 cells treated with a negative-control PPMO of nonsense sequence designated as “scramble” as well as untreated cells that were used as controls. In contrast, no CPE and only small foci of infection were observed in T-ex5 PPMO treated cells at 72 h p.i. (Fig. 3A). To examine SARS-CoV-2 activation and multicycle replication in PPMO treated cells in more detail, Calu-3 cells were treated with PPMO for 24 h prior to infection, then inoculated with virus at a MOI of 0.001 for 1.5 h and incubated for 72 h in the absence of further PPMO, as described above. At different time points virus titers in supernatants were determined by tissue culture infection dose 50 % ($TCID_{50}$) end-point dilution. T-ex5 PPMO treatment dramatically reduced virus titers in Calu-3 cells, by 1,000- and 4,000-fold at 16 and 24 h p.i., respectively, and 180-fold at 48 h p.i. (Fig. 3B).

To confirm knockdown of enzymatically active TMPRSS2 expression, Calu-3 cells were treated with PPMO or remained untreated for 24 h, after which TMPRSS2-specific mRNA was isolated and analysed by RT-PCR as described previously (Böttcher-Friebertshäuser et al., 2011). Total RNA was analysed with primers designed to amplify nucleotides 108 to 1336 of TMPRSS2-mRNA. A full-length PCR product of 1228 bp was amplified from untreated and scramble PPMO treated Calu-3 cells, whereas a shorter PCR fragment of about 1100 bp was amplified from T-ex5 PPMO-treated cells (Fig. 3C). Sequencing revealed that the truncated TMPRSS2-mRNA lacked the entire exon 5 (data not shown). To further confirm that T-ex5 PPMO single dose treatment prior to infection still interferes with TMPRSS2-mRNA splicing at 72 h p.i., total RNA was isolated from infected cells at 72 h p.i. and amplified as described above. As shown in Fig. 3C, the majority of TMPRSS2-mRNA amplified from T-ex5 treated cells at 72 h p.i. lacked exon 5. The data demonstrate that T-ex5 was very effective at producing exon skipping in TMPRSS2-pre-mRNA and, thus, at inhibiting expression of enzymatically active protease, during the virus growth period in Calu-3 cells. However, a small band of the full-length PCR product was visible after 72 h p.i., indicating low levels of expression of enzymatically active TMPRSS2 at later time points of the virus growth period, which may explain the increase in virus titers observed at 48 h p.i. (cf. Fig. 3B). Cell viability was not affected by T-ex5 PPMO treatment of Calu-3 cells, as shown in Fig. 3D and described previously (Böttcher-Friebertshäuser et al., 2011; Limburg et al., 2019).

Together, our data identify TMPRSS2 as host cell factor essential for SARS-CoV-2 activation and multiplication in Calu-3 cells and show that downregulation of TMPRSS2 activity dramatically blocks SARS-CoV-2 replication.

Inhibition of either TMPRSS2 or furin activity suppresses multicycle replication of SARS-CoV-2 in human airway epithelial cells

We next investigated the efficacy of different inhibitors of trypsin-like serine proteases, also inhibiting TMPRSS2, on preventing SARS-CoV-2 activation by TMPRSS2 in Calu-3 cells. We used the natural broad range serine protease inhibitor aprotinin from bovine lung and two prospective peptide mimetic inhibitors of TMPRSS2, MI-432 (Hammami et al., 2012) und MI-1900 (Fig. S1). Aprotinin has long been known to prevent proteolytic activation and multiplication of influenza A virus in cell cultures and mice. Furthermore, inhalation of aerosolized aprotinin by influenza patients markedly reduced the duration of symptoms without causing side effects (Zhirnov et al., 2011). MI-432 was shown to efficiently inhibit proteolytic activation and multiplication of influenza A virus in Calu-3 cells (Meyer et al., 2013). The inhibitor MI-1900 is a monobasic and structurally related analog of the dibasic inhibitor MI-432.

To examine the antiviral efficacy of the protease inhibitors against SARS-CoV-2, Calu-3 cells were infected with the virus at a low MOI of 0.001 for 1.5 h, after which the inoculum was removed and the cells incubated in the presence of the inhibitors at the indicated concentrations for 72 h. The cells were fixed and immunostained using a rabbit antiserum originally produced against SARS-CoV. As shown in Fig. 4, strong CPE and efficient spread of SARS-CoV-2 infection was visible in Calu-3 cells in the absence of protease inhibitors. Spread of SARS-CoV-2 infection and virus induced CPE was efficiently inhibited by aprotinin treatment in a dose-dependent manner and only a few infected cells were visible in Calu-3 cultures treated with 20-50 µM aprotinin. Even at lower concentration of 10 µM the spread of SARS-CoV-2 was greatly reduced and CPE markedly prevented. Treatment with peptide mimetic TMPRSS2 inhibitors MI-432 and MI-1900 also strongly prevented SARS-CoV-2 multiplication and CPE in Calu-3 cells in a dose-dependent manner, although less potently than aprotinin. At 20-50 µM of MI-432 or MI-1900 only small foci of infection were visible. At a concentration of 10 µM, virus spread and CPE in MI-432 treated cells were still markedly reduced compared to control cells, whereas CPE and spread of infection was observed in the presence of 10 µM MI-1900, although still reduced compared to control cells. The data demonstrate that SARS-CoV-2 multiplication in Calu-3 human airway cells can be strongly suppressed by aprotinin and the synthetic TMPRSS2 inhibitors MI-432 and MI-1900.

The observed efficient cleavage of transient expressed SARS-CoV-2 S protein by furin in HEK293 cells prompted us to investigate if furin is involved in SARS-CoV-2 activation in Calu-3 cells. Therefore, virus spread in Calu-3 cells was analysed in the presence of the furin inhibitor MI-1851. Interestingly, MI-1851 strongly inhibited SARS-CoV-2 spread at even the lowest concentration of 10 µM, indicating that furin is critical for SARS-CoV-2 activation and multiplication in these cells (Fig. 4). Finally, to examine whether endosomal cathepsins are involved in SARS-CoV-2 activation in Calu-3 cells, multicycle virus replication was determined in the presence of the cathepsin inhibitor E64d. Cathepsin L was shown to cleave the S protein of 2002 SARS-CoV S close to the S1/S2 site (R667) at T678 *in vitro* (Bosch et al., 2008). Here, strong CPE and foci of infection were observed in E64d-treated cells even at the highest dose of 50 µM, similar to that observed in DMSO-treated as well as untreated control cells, indicating that SARS-CoV-2 activation in Calu-3 cells is independent of endosomal cathepsins.

In sum, our data demonstrate that inhibition of either TMPRSS2 or furin strongly inhibits SARS-CoV-2 in Calu-3 human airway cells, indicating that both proteases are critical for S activation. In contrast, endosomal cathepsins are dispensable or not involved at all in SARS-CoV-2 activation in these cells.

306 *Growth kinetics of SARS-CoV-2 in protease inhibitor-treated Calu-3 cells*

307 To analyse inhibition of SARS-CoV-2 activation and multiplication by the different protease
308 inhibitors in more detail, we performed virus growth kinetics in inhibitor treated cells. Calu-3
309 cells were inoculated with SARS-CoV-2 at a MOI of 0.001 and then incubated in the
310 presence of 10 or 50 µM of the different protease inhibitors. At 16, 24, 48 and 72 h p.i. the
311 viral titer in supernatants was determined by $TCID_{50}$ titration. Untreated cells and cells
312 treated with DMSO alone were used as controls. SARS-CoV-2 replicated to high titers within
313 24-48 h in untreated and DMSO treated cells Calu-3 cells (Fig. 5A). Aprotinin suppressed
314 virus replication 20- to 35-fold compared to control cells even at a concentration of 10 µM.
315 The TMPRSS2 inhibitor MI-432 reduced virus titers in a dose-dependent manner with 5-fold
316 reduction in virus titers at a concentration of 10 µM and 14-fold at 50 µM. Treatment of cells
317 with TMPRSS2 inhibitor MI-1900 reduced virus titers in a manner similar to that of MI-432 at
318 10 µM. However, treatment with 50 µM MI-1900 caused strong inhibition of SARS-CoV-2
319 replication with 25- to 70-fold reduced viral titers compared to control cells. The furin inhibitor
320 MI-1851 efficiently suppressed SARS-CoV-2 multiplication in Calu-3 cells, producing a 30- to
321 75-fold reduction in virus titers at a dose of 10 µM. In contrast, virus multiplication was not
322 affected by treatment with the cathepsin inhibitor E64d, which is in congruence with the data
323 shown in Fig. 4. To provide evidence that inhibition of SARS-CoV-2 replication in inhibitor
324 treated cells was not caused by cytotoxic effects, we analysed cell viability in Calu-3 cells
325 treated with 50 µM of the different inhibitors for 72 h. As shown in Fig. 5B, evaluation of cell
326 viability revealed no significant cytotoxicity by any of the inhibitors under conditions used in
327 the virus growth experiments.

328 The data demonstrate that SARS-CoV-2 replication can be efficiently reduced by inhibiting
329 either TMPRSS2 or furin activity, demonstrating that both proteases are crucial for SARS-
330 CoV-2 activation.

331

332 *Treatment of SARS-CoV-2 infected Calu-3 cells with a combination of TMPRSS2 and furin*
333 *inhibitors*

334 Finally, we wished to examine whether the combination of inhibitors against TMPRSS2 and
335 furin shows a synergistic antiviral effect. Therefore, Calu-3 cells were infected with virus as
336 described above and incubated in the presence of aprotinin, MI-432 or MI-1900 in
337 combination with MI-1851 at 10 and 50 µM each, respectively, for 72 h. Virus titers in
338 supernatants were determined at indicated time points. Single dose treatment of each
339 inhibitor and untreated cells were used as controls. As shown in Fig. 5C, the combination of
340 10 µM of MI-1851 with either aprotinin or MI-432 showed enhanced antiviral activity against

SARS-CoV-2 and 10- to 30-fold reduced virus titers compared to 10 µM of each inhibitior alone and even caused a 4- to 8-fold reduction in virus titer compared to 50 µM single inhibitor treatment. Combination of 50 µM of MI-432 and MI-1851 reduced virus titers 10- to 32-fold compared to 50 µM of each inhibitor alone and thereby dramatically suppressed SARS-CoV-2 multiplication 100- to 250-fold compared to untreated or DMSO treated cells. In contrast, treatment of Calu-3 cells with 50 µM of MI-1851 and aprotinin did not cause further suppression of virus titers compared to the combination of 10 µM of each inhibitor. The combination of 10 µM MI-1851 and MI-1900 did not show enhanced antiviral activity compared to single inhibitor treatments at 10 µM. However, treatment of cells with 50 µM of MI-1900 and MI-1851 caused 5-fold reduction in viral titers when compared to cells treated with 50 µM of each inhibitor alone and thereby dramatically reduced SARS-CoV-2 multiplication in Calu-3 cells compared to control cells. We furthermore examined the antiviral activity of a combination of T-ex5 PPMO and furin inhibitor MI-1851 against SARS-CoV-2 in Calu-3 cells. As shown in Fig. 5D, combined treatment of Calu-3 cells with 25 µM T-ex5 PPMO and 50 µM MI-1851 almost completely blocked SARS-CoV-2 replication with a nearly 40,000-fold reduction in virus titers at 24 h p.i., and reduced virus titers 1,000-fold at 48 h p.i. compared to control cells. Combination of T-ex5 and MI-1851 was synergistic and caused 30- to 10-fold lower virus titers at 16 and 24 h p.i. when compared with single inhibitor treated cells. The data demonstrate that efficient inhibition of S cleavage by a combination of TMPRSS2 and furin inhibitors can block SARS-CoV-2 replication in human airway epithelial cells. Further, our data show that combination of TMPRSS2 and furin inhibitors acts synergistically and allows inhibition of SARS-CoV-2 activation and multiplication at lower doses compared to single protease inhibitor treatment.

In conclusion, our data demonstrate that both TMPRSS2 and furin cleave the SARS-CoV-2 S protein and are essential for virus multicycle replication in Calu-3 human airway cells. The results indicate that TMPRSS2 and furin cleave S at different sites - furin at the S1/S2 site and TMPRSS2 at the S2‘ site - and that TMPRSS2 and furin cannot compensate for each other in SARS-CoV-2 S activation. Hence, inhibition of either one of these critical proteases can render the S protein of SARS-CoV-2 unable to efficiently mediate virus entry and membrane fusion. Therefore, TMPRSS2 and furin provide promising drug targets for treatment of COVID-19, and inhibitors MI-432, MI-1900, MI-1851 as well as T-ex5 PPMO may provide the basis for development of novel protease inhibitors. Our data further demonstrate that aprotinin efficiently prevents proteolytic activation and multiplication of SARS-CoV-2 in human airway cells and is therefore worthy of consideration for further testing and possible development as a therapeutic treatment for COVID-19.

Discussion

Proteolytic processing of CoV S is a complex process that requires cleavage at two different sites and is yet not fully understood. The amino acid sequence at the S1/S2 and S2' cleavage sites varies among CoVs (Fig. 1B), suggesting that partially different proteases may be involved in activation. Sequence analyses of the S protein of the novel emerged SARS-CoV-2 suggested that the R-R-A-R motif at the S1/S2 site may by sensitive to cleavage by furin, while the S2' site contains a single R residue that can be cleaved by trypsin-like serine proteases such as TMPRSS2 (Coutard et al., 2020; Walls et al., 2020; Hoffmann et al., 2020). In the present study, we demonstrate that the SARS-CoV-2 S protein is cleaved by furin and by TMPRSS2. Furthermore, we show that multicycle replication of SARS-CoV-2 in Calu-3 human airway cells is strongly suppressed by inhibiting TMPRSS2 and furin activity, demonstrating that both proteases are crucial for S activation in these cells. Our data indicate that furin cleaves at the S1/S2 site, whereas TMPRSS2 cleaves at the S2' site. The effective processing of the S1/S2 site by furin was additionally confirmed by comparing the cleavage rates of various FRET substrates derived from the P6-P3' segments of SARS-CoV-2 and other CoVs. The data clearly revealed that due to the 4-mer PRRA insertion a well suited furin cleavage site exists in S of SARS-CoV-2, which is similarly cleaved as the sequence from the IBV CoV, whereas the analogous substrate of SARS-CoV is not processed by furin. Strong inhibition of SARS-CoV-2 replication in Calu-3 cells by synthetic furin inhibitor MI-1851 furthermore suggests that TMPRSS2 does not compensate for furin cleavage at the S1/S2 site. Likewise, strong inhibition of SARS-CoV-2 replication by knockdown of TMPRSS2 activity using T-ex5 PPMO or treatment of Calu-3 cells with aprotinin, MI-432 and MI-1900, respectively, indicates that furin cannot compensate for the lack of TMPRSS2 in S activation. This was further confirmed by using an analogous FRET substrate derived from the S2' cleavage site of the SARS-CoV-2 S protein (Fig. S2). Kinetic measurements clearly revealed that this substrate cannot be cleaved by furin (Fig. S2). Thus, we could experimentally demonstrate for the first time that furin only activates the S1/S2 site, as expected from the amino acid sequence at the cleavage sites (Coutard et al., 2020; Walls et al., 2020). Together, our data indicate that furin and TMPRSS2 cleave S at different sites, and, cleavage by both proteases is crucial to render the S protein active for mediating virus entry and membrane fusion (Fig. 6). Iwata-Yoshikawa et al. showed that TMPRSS2-deficient mice do not suffer from pathology when infected with SARS-CoV and MERS-CoV (Iwata-Yoshikawa et al., 2019). The data demonstrated that TMPRSS2 is essential for multicycle replication and spread of these CoVs similar to what we and others have been observed for certain influenza A virus strains (Hatesuer et al., 2013; Tarnow et al., 2014; Sakai et al., 2014). However, it remains to be determined whether knockout of TMPRSS2 prevents cleavage of the S proteins of SARS-CoV and MERS-CoV at both sites, S1/S2 and S2', or

whether another protease is involved in S cleavage similar to what we have observed here for SARS-CoV-2.

In cell culture, CoVs can enter cells via two distinct routes: the late endosome where S is cleaved by cathepsins or via the cell-surface or early endosome utilizing trypsin-like proteases for S cleavage (Simmons et al., 2005; Bosch et al., 2008; reviewed in Millet and Whittaker, 2015). However, several recent studies revealed that clinical isolates of human CoV (HCoV) achieve activation by trypsin-like serine proteases and utilize endosomal cathepsins only in the absence of suitable trypsin-like proteases in cell culture (Shirato et al., 2016, 2018). Thus, activation by cathepsins appears to be a mechanism that is acquired by the virus during multiple passaging in cell cultures (Shirato et al., 2018). Congruently, Zhou et al. showed that SARS-CoV pathogenesis in mice was strongly prevented by camostat, a broad-range inhibitor of trypsin-like serine proteases, but not by inhibitors of endosomal cathepsins (Zhuo et al., 2015). Here, we show that the cysteine protease inhibitor E64d that also inhibits cathepsin L and B did not affect SARS-CoV-2 replication in Calu-3 cells, indicating that endosomal cathepsins are dispensable or not involved at all in SARS-CoV-2 activation in human airway cells.

The presence of a multibasic cleavage site that is processed by ubiquitously expressed furin and, therefore, supports systemic spread of infection, has long been known to be a major determinant of the pathogenicity of HPAIV in poultry (reviewed in Garten and Klenk, 2008). In contrast, the HA of LPAIV is activated at a monobasic cleavage site by trypsin-like serine proteases present in a limited number of tissues limiting spread of infection to these tissues. The S protein of IBV strain Beaudette contains multibasic motifs at the S1/S2 and S2' site (Fig. 1B). IBV belongs to the genus *Gammacoronavirus* and causes a highly contagious, acute respiratory disease of chickens. Cleavage of IBV S protein by furin at the S2' site has been associated with neurotropism in chicken (Cheng et al., 2019). Congruently, here, FRET substrates of the S1/S2 and S2' site of the IBV Beaudette S protein were efficiently cleaved by furin (Fig. 2B and Fig. S2B). However, the advantage of furin-cleavable multibasic motifs at the S1/S2 and/or S2' site for multicycle replication, cellular tropism and pathogenicity of HCoVs remains to be determined. HCoV-OC43 and HCoV-HKU1 possess a furin cleavage motif at the S1/S2 site. In contrast, the S proteins of the 2002 SARS-CoV, HCoV-229E and HCoV-NL63 possess single arginine residues at both cleavage sites (see also Fig. 2B and S2A). Interestingly, among the S proteins of the seven CoV infecting humans only SARS-CoV S lacks the 4-mer insertion at the S1/S2 site (Fig. 1B; Walls et al., 2020). The S protein of MERS-CoV contains a dibasic motif of the sequence R-X-X-R at both S1/S2 and S2' site. It is still controversial whether MERS-CoV is activated by furin in human airway epithelial cells, as its clear role remains to be demonstrated (Gierer et al., 2015; Millet and Whittaker,

2014; Burkhard et al., 2014; Matsuyama et al., 2018). Probably, other proteases like the serine protease matriptase/ST14, which also prefers sequences with arginine in P1 and P4 position, might be involved. Matriptase is expressed in a broad range of cells and tissues and has been shown to activate the HA of H9N2 influenza A viruses possessing the cleavage site motif R-S-S-R (Baron et al., 2013; reviewed in Böttcher-Friebertshäuser, 2018). Interestingly, a study by Park et al. indicated that cleavage of MERS-CoV S by furin or other PCs at the S1/S2 site takes place in virus-producing cells prior to virus release and can impact the cellular localization of membrane fusion and virus entry into a new cell (Park et al., 2016). Cleavage of MERS-CoV at the S1/S2 site was postulated as a prerequiste for subsequent cleavage of S at the S2' site by host proteases present at the surface or in early endosomes of human airway cells facilitating virus entry independent of S cleavage by cathepsins in the late endosome. However, other HCoV including the 2002 SARS-CoV are described to be released with non-cleaved S from the infected cell. Hence, S cleavage at both sites, S1/S2 and S2', has to take place at the stage of entry for these viruses.

The present study demonstrates that TMPRSS2 and furin are promising drug targets for the treatment of COVID-19 either by targeting one of these proteases alone or by a combination of furin and TMPRSS2 inhibitors. The used TMPRSS2 inhibitors MI-432 and MI-1900 as well as the furin inhibitor MI-1851 provide promising compounds for further drug development. In search for suitable antiviral therapies against SARS-CoV-2 infections, protease inhibitors that have been approved for other applications may be promising for drug repurposing to treat COVID-19. Aprotinin is a broad range serine protease inhibitor isolated from bovine lung, which is used as a fibrinolysis inhibitor to reduce perioperative bleeding (reviewed in Steinmetzer et al., 2020) and has long been known to inhibit influenza A virus activation and replication in cell culture and in mice *in vivo* (Zhirnov et al., 2011). In a clinical trial, inhalation of aerosolized aprotinin in patients with influenza and parainfluenza markedly reduced the duration of symptoms without causing side effects (Zhirnov et al., 2011). Thus, aprotinin is an inhibitor of TMPRSS2 worthy of consideration for further testing and possible development as a therapeutic treatment for COVID-19. Another promising TMPRSS2 inhibitor candidate for COVID-19 treatment is the broad range protease inhibitor camostat. Camostat mesylate is a phenyl-4-guanidinobenzoate derivative originally developed under the name FOY-305 for the treatment of pancreatitis (Tanaka et al., 1979; Midgley et al., 1994) and has been shown to efficiently inhibit replication of different CoV in cell culture and experimentally infected mice (Kawase et al., 2012; Shirato et al., 2013; Zhou et al., 2015). Recently, Hoffmann et al. showed that pretreatment of human Caco-2 colon cells and human airway cells with camostat mesylate markedly reduced entry of SARS-CoV-2 as well as VSV pseudotypes containing the SARS-CoV-2 S protein (Hoffmann et al., 2020).

However, it should be noted that all of these compounds inhibit numerous trypsin-like serine proteases and thus may cause various adverse effects. A specific inhibition of TMPRSS2 activity during an acute SARS-CoV-2 infection would provide the most promising approach to reduce side effects by inhibiting virus activation by host cell proteases. TMPRSS2-deficient mice show no discernible phenotype, indicating functional redundancy or compensation of physiological functions by other protease(s) in the host (Kim et al., 2006). Unfortunately, there is no crystal structure of TMPRSS2 available so far, which prohibits a rational structure-based design of more efficient inhibitors of this protease. However, first homology models have been established, which may help for the development of improved TMPRSS2 inhibitors in the future (Steinmetzer and Hardes, 2018*; Rensi et al. https://chemrxiv.org*).

PPMO are highly selective inhibitors of target gene expression. They bind to a complementary sequence in target mRNA and can affect gene expression by steric blockage of translation initiation or pre-mRNA splicing. The demonstration of T-ex5 PPMO efficacy in the present study suggests that reducing TMPRSS2 expression by use of a mRNA-directed approach in general and by PPMO in particular is worthy of further consideration. Importantly, in various experimental animal models of other viral infections and disease, PPMO were able to be transported to lung tissue after intranasal administration and produced strong reductions in virus growth and virus-induced pathology (Gabriel et al., 2008; Lupfer et al,. 2008, Lai et al,. 2008; Opriessnig et al., 2011).

Very effective furin inhibitors containing a C-terminal 4-amidinobenzylamide residue have been developed in recent years. Several of these analogues have been successfully used to inhibit the replication of numerous furin dependent human pathogenic viruses like H5N1 influenza A virus, Chikungunya virus, West-Nile virus and Dengue-2 virus, Mumps virus or respiratory syncytial virus (RSV) (reviewed in Steinmetzer and Hardes, 2018; Krüger et al., 2018; Van Lam van et al., 2019). So far, these inhibitors have only been used in virus infected cell cultures, but not in animal models. However, the less potent furin inhibitor hexa-D-arginine has been used in mice and rats to protect them against *Pseudomonas aeruginosa* Exotoxin A and anthrax toxemia (Sarac et al., 2002, 2004). Therefore, it can be speculated that a specific furin inhibition in the respiratory tract and lung by inhalative treatment of e.g. MI-1851 or structurally related compounds could be possible without severe side reactions, despite many physiological functions of furin.

Here, the combination of the TMPRSS2 inhibitors aprotinin or MI-432 with furin inhibitor MI-1851 showed enhanced antiviral activity against SARS-CoV-2 in human airway cells and supported strong reduction of virus multiplication at lower doses compared to treatment with each inhibitor alone. Therefore, the combination of TMPRSS2 and furin inhibitors provides a promising therapeutic strategy for treatment of SARS-CoV-2 infections that not only may

enhance antiviral effects, but may also reduce drug toxicity and undesirable side effects by allowing reductions of the inhibitor doses. Notably, inhibition of TMPRSS2 and furin acts on the same target and our data show that inhibition of S cleavage at one of the two sites is sufficient to suppress SARS-CoV-2 replication by reduced production of infectious progeny virus containing inactive S. Thus, the combination of TMPRSS2 and furin inhibitors can act synergistically until S cleavage at one or two sites is completely prevented. The combination of protease inhibitors with antiviral compounds provides an approach that may show even more synergistic antiviral activity at lower drug doses and may furthermore exclude the development of drug resistant viruses. The combination of TMPRSS2 and furin inhibitors, respectively, with the neuraminidase inhibitor oseltamivir carboxylate has been shown to block influenza A virus replication in human airway cells at remarkably lower concentration of each inhibitor as compared to single inhibitor treatment (Böttcher-Friebertshäuser et al., 2012). Combination of a furin inhibitor with oseltamivir carboxylate and the antiviral compounds ribavirin and favipiravir, respectively, efficiently blocked multicycle replication of HPAIV of subtype H5N1 and H7N1 in cell cultures (Lu et al., 2015; Garten et al., 2015). Thus, combination of protease inhibitors (e.g. aprotinin or camostat) and antivirals provides a promising approach to block SARS-CoV-2 replication that should be tested in cell cultures and animal models and should furthermore be considered as therapeutic strategy for the treatment of COVID-19.

In summary, we demonstrate that TMPRSS2 and furin are essential for activation and multiplication of the novel emerged SARS-CoV-2 in human airway epithelial cells and provide promising drug targets for treatment of COVID-19. TMPRSS2 and furin have been shown to be involved in the proteolytic activation of a broad range of viruses. However, the development of host protease inhibitors as a preventative and/or therapeutic strategy for the treatment of virus infections has been minimal to date. Our data demonstrate the high potential of protease inhibitors as drugs for SARS-CoV-2 treatment and highlight the urgent need of drug development and repurposing of potent host protease inhibitors for the treatment of virus infections in general and emerging CoV infections in particular.

Acknowledgement

We are grateful to Christian Drosten for providing the virus. We thank Iris Lindberg for providing recombinant furin. This work was funded by the LOEWE Center DRUID (project D1), by the German Center for Infection Research (DZIF), and by the Deutsche Forschungsgemeinschaft (DFG, German Research Foundation) SFB 1021 (project B07). We thank Diana Kruhl for excellent technical assistance.

Materials and Methods

Cells. Calu-3 human airway epithelial cells (ATCC® HTB55) were cultured in Dulbecco's modified Eagle's medium (DMEM)-Ham F-12 medium (1:1) (Gibco) supplemented with 10% fetal calf serum (FCS), penicillin, streptomycin, and glutamine, with fresh culture medium replenished every 2 to 3 days. Vero E6 (ATCC® CRL-1586) and HEK293 (ATCC® CRL-1573) cells were maintained in DMEM supplemented with 10 % FCS, antibiotics and glutamine.

Virus and plasmids. Experiments with SARS-CoV-2 were performed under biosafety level 3 (BSL-3) conditions. The virus used in this study was SARS-CoV-2 isolate Munich 929 (kindly provided by Christian Drosten, Institute of Virology, Charité Universitätsmedizin Berlin, Germany). Virus stock was propagated on Vero E6 cells in DMEM medium with 1 % FCS for 72 h. Cell supernatant was cleared by low-speed centrifugation and stored at -80°C.
The cDNA encoding the SARS-CoV-2 spike protein of isolate Wuhan-Hu-1 (GenBank accession number MN908947; codon-optimized, sequence available upon request) with a C-terminal Myc-6xHis-tag was synthesized at Eurofins and subcloned into in the pCAGGS expression plasmid using XhoI and NheI restriction sites (pCAGGS-S-Myc-6xHis). Expression plasmid pCAGGS-TMPRSS2 encoding the cDNA of human TMPRSS2 has been described previously (Böttcher et al., 2006).

Antibodies. A polyclonal serum against 2002 SARS-CoV was generated by immunization of rabbits with inactivated SARS-CoV. A monoclonal mouse antibody against the C-terminal Myc-tag was purchased from CellSignaling Technology (2276S). A monoclonal mouse anti-beta actin antibody was purchased from Abcam (ab6276). Horseradish peroxidase (HRP)-conjugated secondary antibodies were purchased from DAKO.

PPMO. Phosphorodiamidate morpholino oligomers (PMO) were synthesized at Gene Tools LLC (Corvallis, OR, USA). PMO sequences (5` to 3`) were CAGAGTTGGAGCACTTGCTGCCCA for T-ex5 and CCTCTTACCTCAGTTACAATTTATA for scramble. The cell-penetrating peptide (RXR)4 (where R is arginine and X is 6-aminohexanoic acid) was covalently conjugated to the 3` end of each PMO through a noncleavable linker, to produce peptide-PMO (PPMO), by methods described previously (Abes et al., 2006).

Protease inhibitors. Aprotinin was purchased from AppliChem, the cysteine protease inhibitor E64d from Sigma-Aldrich (E8640). The synthetic inhibitors of TMPRSS2 and furin were synthesized according to previous methods (Hammami et al., 2012; Hardes et al., 2015). Stock solutions of protease inhibitors were prepared in double distilled water (aprotinin, MI-432, MI-1851) or sterile DMSO (MI-1900, E64d) and stored at -20°C.

Synthesis of FRET substrates

The peptides were synthesized by automated solid phase peptide synthesis on a Syro 2000 synthesizer (MultiSynTech GmbH, Witten, Germany) using approximately 100 mg Rink-amide-MBHA resin (loading 0.68 mmol/g) for each 2 ml reaction vessel and a standard Fmoc-protocol with double couplings (approximately 4-fold excess of Fmoc amino acid, HOBt and HBTU, respectively, and 8 equiv. DIPEA, 2 × 2 h coupling time) as described recently (Hardes et al., 2013). After final coupling of Boc-2-aminobenzoic acid, the resin was washed with 20 % piperidine in DMF (5 and 15 min) to remove an acylation on the 3-nitrotyrosine (Singh et al., 2002). The peptides were cleaved from the resin and deprotected by a mixture of TFA/triisopropylsilane/water (95/2.5/2.5, v/v/v) over 2 h at room temperature, followed by precipitation in cold diethyl ether. All peptides were purified by preparative reversed-phase HPLC to more than 95 % purity based on the detection at 220 nm, and finally obtained as lyophilized TFA-salts.

Enzyme kinetic measurements with recombinant soluble human furin

The measurements were performed in black 96-well plates (Nunc, Langenselbold) at room temperature with a microplate reader (Safire2, Tecan, Switzerland) at λ_{ex} 320 nm and λ_{em} 405 nm. Each well contained 20 µL of the substrate solution (dissolved in water), and 150 µL buffer (100 mM HEPES, 0.2 % Triton X-100, 2 mM $CaCl_2$, 0.02 % Natriumazid und 1 mg/mL BSA, pH 7.0). The measurements were started by addition of 20 µL furin (Kacprzak et al., 2004) solution (0.5 nM in assay). The measurements were performed for 5 min, and the steady-state rates were calculated from the slopes of the progress curves.

RNA isolation, RT-PCR analysis of exon skipping, and RT-qPCR analysis of protease transcripts. For analysis of TMPRSS2-mRNA from PPMO-treated Calu-3 cells, cells were incubated with the indicated concentrations (25 µM) of T-ex5 or scramble PPMO or without PPMO in PPMO medium (DMEM supplemented with 0.1 % BSA, antibiotics, and glutamine) for 24 h. Total RNA was isolated at the indicated time points using the RNeasy Mini kit (QIAGEN) according to the manufacturer's protocol. Reverse transcription-PCR (RT-PCR) was carried out with total RNA using the one-step RT-PCR kit (QIAGEN) according to the supplier's protocol. To analyse-TMPRSS2 mRNAs for exon skipping, primers TMPRSS2-

629 108fwd (5`-CTA CGA GGT GCA TCC-3`) and TMPRSS2-1336rev (5`-CCA GAG GCC CTC
630 CAG CGT CAC CCT GGC AA-3`), designed to amplify a full-length PCR product of 1,228 bp
631 from control cells and a shorter PCR fragment of about 1,100 bp lacking exon 5 from T-ex5-
632 treated cells (Böttcher-Friebertshäuser et al., 2011) were used. RT-PCR products were
633 resolved on a 0.8 % agarose gel stained with ethidium bromide.
634
635 **Infection of cells and multicycle virus replication in the presence of protease inhibitors**
636 **or PPMO.** SARS-CoV-2 infection experiments of Calu-3 cells were performed in serum-free
637 DMEM supplemented with glutamine and antibiotics (DMEM++). For analysis of multicycle
638 replication kinetics Calu-3 cells were seeded in 12-well plates and grown to 90 % confluence.
639 Cells were then inoculated with virus at a multiplicity of infection (MOI) of 0.001 in DMEM++
640 for 1.5 h, washed with PBS, and incubated in DMEM supplemented with 3 % FCS, glutamine
641 and antibiotics (DMEM+++) with or without addition of protease inhibitors or DMSO to the
642 medium for 72 h. At 16, 24, 48, and 72 h postinfection (p.i.), supernatants were collected,
643 and viral titers were determined by tissue culture infection dose 50 % ($TCID_{50}$) titration as
644 described below. In addition, cells were fixed and immunostained against viral proteins as
645 described below at 72 h p.i. to evaluate virus spread and virus-induced CPE.
646 For PPMO treatment, Calu-3 cells were incubated with 25 µM T-ex5 or scramble PPMO or
647 remained untreated in PPMO medium for 24 h prior to infection. Cells were infected as
648 described above and incubated in DMEM+++ without PPMO for 72 h.
649
650 **Virus titration by $TCID_{50}$.** Viral supernatants were serial diluted in DMEM++. Each infection
651 time point was titrated in 4 replicates from 5^{1} to 5^{11}. Subsequently, 100 µl of each virus
652 dilution were transfered to Calu-3 cells grown in 96-well plates containing 100 µl DMEM+++
653 and incubated for 72 h. Viral titers were determined with Spearman and Kärber algorithm
654 described in Hierholzer and Killington et al., 1996.
655
656 **Transient expression of SARS CoV-2 S protein in HEK293 cells.** For transient expression
657 of SARS-CoV-2 S protein 60 % confluent HEK293 cells were co-transfected with 1.6 µg of
658 pCAGGS-S-Myc-6xHis and either 15 ng of empty pCAGGS vector or pCAGGS-TMPRSS2
659 using Liopfectamine® 2000 (Invitrogen) according to the manufacturers protocol for 48 h.
660 Cells were harvested and centrifuged for 5 min at 8.000 x g. Subsequently cells were
661 subjected to SDS-PAGE and Western blot analysis as described below.
662
663 **SDS-PAGE and Western blot analysis**. Cells were washed with PBS, lysed in CelLytic™ M
664 buffer (Sigma Aldrich) with a protease inhibitor cocktail (Sigma Aldrich, P8340), resuspended
665 in reducing SDS-PAGE sample buffer, and heated at 95 °C for 10 min. Proteins were

subjected to SDS-PAGE (10 % acrylamid gel), transferred to a polyvinylidene difluoride (PVDF) membrane (GE Healthcare), and detected by incubation with primary antibodies and species-specific peroxidase-conjugated secondary antibodies. Proteins were visualized using the ChemiDoc XRS system with Image Lab software (Bio-Rad).

Immunohistochemical staining and microscopy. To visualize viral spread in SARS-CoV-2 infected Calu-3 cells, immunohistochemical staining was performed. Calu-3 cells were fixed 72 h post infection in 4 % paraformaldehyde (PFA) for 36 h at 4 °C. The cells were permeabilized with 0.3 % Triton-X-100 (Sigma Aldrich) for 20 min at room temperature (RT). The cells were incubated with a polyclonal rabbit serum against 2002 SARS-CoV for 1.5 h at RT, a species-specific peroxidase-conjugated secondary antibody for 1 h at RT and subsequently stained using the peroxidase substrate KPL TrueBlue™ (Seracare) and further analysed on a Leica Dmi1 microscope.

Cell viability assay. Cell viability was assessed by measuring the cellular ATP content using the CellTiterGlo® luminescent cell viability assay (Promega). Calu-3 cells grown in 96-well plates were incubated with 25 µM of each PPMO or 50 µM of each of the protease inhibitors for 24 and 72 h, respectively. Subsequently, cells were incubated with the substrate according to the manufacturer's protocol. Luminescence was measured using a 96-well plate (Nunc) with a luminometer (Centro LB 960; Berthold Technologies). The absorbance values of PPMO- or inhibitor-treated cells were converted to percentages by comparison to untreated control cells, which were set at 100 % cell viability.

690 **References**

691

692 Abes S, Moulton HM, Clair P, Prevot P, Youngblood DS, Wu RP, Iversen PL, Lebleu B. 2006.
693 Vectorization of morpholino oligomers by the (R-Ahx-R)4 peptide allows efficient splicing correction in
694 the absence of endosomolytic agents. J Control Release 116:304-13.

695 Baron J, Tarnow C, Mayoli-Nüssle D, Schilling E, Meyer D, Hammami M, Schwalm F, Steinmetzer T,
696 Guan Y, Garten W, Klenk HD, Böttcher-Friebertshäuser E. 2013. Matriptase, HAT, and TMPRSS2
697 activate the hemagglutinin of H9N2 influenza A viruses. J Virol 87:1811-20.

698 Belouzard S, Chu VC, Whittaker GR. 2009. Activation of the SARS coronavirus spike protein via
699 sequential proteolytic cleavage at two distinct sites. Proc Natl Acad Sci U S A 106:5871-6.

700 Bosch BJ, Bartelink W, Rottier PJ. 2008. Cathepsin L functionally cleaves the severe acute respiratory
701 syndrome coronavirus class I fusion protein upstream of rather than adjacent to the fusion peptide. J
702 Virol 82:8887-90.

703 Böttcher E, Matrosovich T, Beyerle M, Klenk HD, Garten W, Matrosovich M. 2006. Proteolytic
704 activation of influenza viruses by serine proteases TMPRSS2 and HAT from human airway epithelium.
705 J Virol 80:9896-8.

706 Böttcher-Friebertshäuser E, Lu Y, Meyer D, Sielaff F, Steinmetzer T, Klenk HD, Garten W. 2012.
707 Hemagglutinin activating host cell proteases provide promising drug targets for the treatment of
708 influenza A and B virus infections. Vaccine 30:7374-80.

709 Böttcher-Friebertshäuser E, Stein DA, Klenk HD, Garten W. 2011. Inhibition of influenza virus infection
710 in human airway cell cultures by an antisense peptide-conjugated morpholino oligomer targeting the
711 hemagglutinin-activating protease TMPRSS2. J Virol 85:1554-62.

712 Böttcher-Friebertshäuser E. 2018. Membrane-Anchored Serine Proteases: Host Cell Factors in
713 Proteolytic Activation of Viral Glycoproteins. In: Böttcher-Friebertshäuser E., Garten W., Klenk H. (eds)
714 Activation of Viruses by Host Proteases. Springer, Cham, p.153-203. Review.

715 Bugge TH, Antalis TM, Wu Q. Type II transmembrane serine proteases. 2009. J Biol Chem
716 284:23177-81. Review.

717 Burkard C, Verheije MH, Wicht O, van Kasteren SI, van Kuppeveld FJ, Haagmans BL, Pelkmans L,
718 Rottier PJ, Bosch BJ, de Haan CA. 2014. Coronavirus cell entry occurs through the endo-/lysosomal
719 pathway in a proteolysis-dependent manner. PLoS Pathog 10:e1004502.

720 Cheng J, Zhao Y, Xu G, Zhang K, Jia W, Sun Y, Zhao J, Xue J, Hu Y, Zhang G. 2019. The S2 Subunit
721 of QX-type Infectious Bronchitis Coronavirus Spike Protein Is an Essential Determinant of
722 Neurotropism. Viruses 11:pii: E972.

723 Coutard B, Valle C, de Lamballerie X, Canard B, Seidah NG, Decroly E. 2020. The spike glycoprotein
724 of the new coronavirus 2019-nCoV contains a furin-like cleavage site absent in CoV of the same
725 clade. Antiviral Res 176:104742.

726 Follis KE, York J, Nunberg JH. 2006. Furin cleavage of the SARS coronavirus spike glycoprotein
727 enhances cell-cell fusion but does not affect virion entry. Virology 350:358-69.

728 Gabriel G, Nordmann A, Stein DA, Iversen PL, Klenk HD. 2007. Morpholino Oligomers Targeting PB1
729 and NP Genes Enhance Survival of Mice Infected with Highly Pathogenic Influenza A H7N7 Virus.
730 Journal of General Virology 89:939-48.

731

732 Garten W, Braden C, Arendt A, Peitsch C, Baron J, Lu Y, Pawletko K, Hardes K, Steinmetzer T,
733 Böttcher-Friebertshäuser E. 2015. Influenza virus activating host proteases: Identification, localization
734 and inhibitors as potential therapeutics. Eur J Cell Biol 94:375-83.

735 Garten W, Klenk HD. 2008. Cleavage activation of the influenza virus hemagglutinin and its role in
736 pathogenesis. In: Klenk HD, Matrosovich MN, Stech J (eds) Avian Influenza. Karger, Basel, pp 156-
737 167. Review.

738 Garten, W. 2018. Characterization of Proprotein Convertases and Their Involvement in Virus
739 Propagation. In: Böttcher-Friebertshäuser E., Garten W., Klenk H. (eds) Activation of Viruses by Host
740 Proteases. Springer, Cham, p.205-248. Review.

741 Gierer S, Müller MA, Heurich A, Ritz D, Springstein BL, Karsten CB, Schendzielorz A, Gnirß K,
742 Drosten C, Pöhlmann S. 2015. Inhibition of proprotein convertases abrogates processing of the middle
743 eastern respiratory syndrome coronavirus spike protein in infected cells but does not reduce viral
744 infectivity. J Infect Dis 211:889-97.

745 Hammami M, Rühmann E, Maurer E, Heine A, Gütschow M, Klebe G, Steinmetzer T. 2012. New 3-
746 amidinophenylalanine-derived inhibitors of matriptase. MedChemComm 3:807-13.

747 Hardes K, Becker GL, Lu Y, Dahms SO, Köhler S, Beyer W, Sandvig K, Yamamoto H, Lindberg I,
748 Walz L, von Messling V, Than ME, Garten W, Steinmetzer T. 2015. Novel furin inhibitors with potent
749 anti-infectious activity. ChemMedChem 10:1218-31.

750 Hardes K, Zouhir Hammamy M, Steinmetzer T. 2013. Synthesis and characterization of novel
751 fluorogenic substrates of coagulation factor XIII-A. Anal Biochem 442:223-30.

752 Hatesuer B, Bertram S, Mehnert N, Bahgat MM, Nelson PS, Pöhlmann S, Schughart K. 2013.
753 Tmprss2 is essential for influenza H1N1 virus pathogenesis in mice. PLoS Pathog 9:e1003774.

754 Heald-Sargent T, Gallagher T. Ready, set, fuse! 2012. The coronavirus spike protein and acquisition
755 of fusion competence. Viruses 4:557-80.

756 Hierholzer JC, Killington RA. 1996. Virus Isolation and Quantitation. In: Mahy BWJ, Kangro HO, (eds).
757 Virology Methods Manual. London, San Diego: Academic Press. pp. 24–32.

758 Hoffmann M, Hofmann-Winkler H, Pöhlmann S. 2018. Priming Time: How Cellular Proteases Arm
759 Coronavirus Spike Proteins. In: Böttcher-Friebertshäuser E., Garten W., Klenk H. (eds) Activation of
760 Viruses by Host Proteases. Springer, Cham, p.71-98. Review.

761 Hoffmann M, Kleine-Weber H, Schroeder S, Krüger N, Herrler T, Erichsen S, Schiergens TS, Herrler
762 G, Wu NH, Nitsche A, Müller MA, Drosten C, Pöhlmann S. 2020. SARS-CoV-2 Cell Entry Depends on
763 ACE2 and TMPRSS2 and Is Blocked by a Clinically Proven Protease Inhibitor. Cell. pii: S0092-
764 8674(20)30229-4.

765 Iwata-Yoshikawa N, Okamura T, Shimizu Y, Hasegawa H, Takeda M, Nagata N. 2019. TMPRSS2
766 Contributes to Virus Spread and Immunopathology in the Airways of Murine Models after Coronavirus
767 Infection. J Virol 93:e01815-18.

768 Kacprzak MM, Peinado JR, Than ME, Appel J, Henrich S, Lipkind G, Houghten RA, Bode W, Lindberg
769 I. 2004. Inhibition of furin by polyarginine-containing peptides: nanomolar inhibition by nona-D-
770 arginine. J Biol Chem 279:36788-94.

771 Kassell B, Radicevic M, Ansfield MJ, Laskowski M. 1965. The basic trypsin inhibitor of bovine
772 pancreas. IV. The linear sequence of the 58 amino acids. Biochem. Biophys. Res. Commun 18: 255-8.

773 Kawase M, Shirato K, van der Hoek L, Taguchi F, Matsuyama S. 2012. Simultaneous treatment of
774 human bronchial epithelial cells with serine and cysteine protease inhibitors prevents severe acute
775 respiratory syndrome coronavirus entry. J Virol 86:6537-45.

776 Kim TS, Heinlein C, Hackman RC, Nelson PS. 2006. Phenotypic analysis of mice lacking the
777 Tmprss2-encoded protease. Mol Cell Biol 26:965-75.

778 Klenk HD, Garten W. 1994. Host cell proteases controlling virus pathogenicity. Trends Microbiol 2:39-
779 43.

780 Krüger N, Sauder C, Huttl S, Papies J, Voigt K, Herrler G, Hardes K, Steinmetzer T, Orvell C, Drexler
781 JF, Drosten C, Rubin S, Müller MA, Hoffmann M. 2018. Entry, Replication, Immune Evasion, and
782 Neurotoxicity of Synthetically Engineered Bat-Borne Mumps Virus. Cell reports 25:312-20.

783 Lai SH, Stein DA, Guerrero-Plata A, Liao SL, Ivanciuc T, Hong C, Iversen PL, Casola A, Garofalo RP.
784 2008. Inhibition of Respiratory Syncytial Virus Infections with Morpholino Oligomers in Cell Cultures
785 and in Mice. Molecular Therapy 16:1120-8.
786
787 Limburg H, Harbig A, Bestle D, Stein DA, Moulton HM, Jaeger J, Janga H, Hardes K, Koepke J,
788 Schulte L, Koczulla AR, Schmeck B, Klenk HD, Böttcher-Friebertshäuser E. 2019. TMPRSS2 Is the
789 Major Activating Protease of Influenza A Virus in Primary Human Airway Cells and Influenza B Virus in
790 Human Type II Pneumocytes. J Virol 93:pii: e00649-19.

791 Lu Y, Hardes K, Dahms SO, Böttcher-Friebertshäuser E, Steinmetzer T, Than ME, Klenk HD, Garten
792 W. 2015. Peptidomimetic furin inhibitor MI-701 in combination with oseltamivir and ribavirin efficiently
793 blocks propagation of highly pathogenic avian influenza viruses and delays high level oseltamivir
794 resistance in MDCK cells. Antiviral Res 120:89-100.

795 Lupfer C, Stein DA, Mourich DV, Tepper SE, Iversen PL, Pastey M. 2008. Inhibition of Influenza A
796 H3N8 Infections in Mice by Morpholino Oligomers. Archives of Virology 153:929-37.
797
798 Madu IG, Roth SL, Belouzard S, Whittaker GR. 2009. Characterization of a highly conserved domain
799 within the severe acute respiratory syndrome coronavirus spike protein S2 domain with characteristics
800 of a viral fusion peptide. J Virol 83:7411-21.

801 Matsuyama S, Shirato K, Kawase M, Terada Y, Kawachi K, Fukushi S, Kamitani W. 2018. Middle East
802 Respiratory Syndrome Coronavirus Spike Protein Is Not Activated Directly by Cellular Furin during
803 Viral Entry into Target Cells. J Virol 92:pii: e00683-18.

804 Meyer D, Sielaff F, Hammami M, Böttcher-Friebertshäuser E, Garten W, Steinmetzer T. 2013.
805 Identification of the first synthetic inhibitors of the type II transmembrane serine protease TMPRSS2
806 suitable for inhibition of influenza virus activation. Biochem J 452:331-43.

807 Midgley I, Hood AJ, Proctor P, Chasseaud LF, Irons SR, Cheng KN, Brindley CJ, Bonn R. 1994.
808 Metabolic fate of 14C-camostat mesylate in man, rat and dog after intravenous administration.
809 Xenobiotica 24:79-92.

810 Millet JK, Whittaker GR. 2015. Host cell proteases: Critical determinants of coronavirus tropism and
811 pathogenesis. Virus Res 202:120-34. Review.

812 Moulton HM, Moulton JD. 2010. Morpholinos and their peptide conjugates: therapeutic promise and
813 challenge for Duchenne muscular dystrophy. Biochim Biophys Acta 1798:2296-2303. Review.

814 Opriessnig T, Patel D, Wang R, Halbur PG, Meng XJ, Stein DA, Zhang YJ. 2011. Inhibition of Porcine
815 Reproductive and Respiratory Syndrome Virus Infection in Piglets by a Peptide-Conjugated
816 Morpholino Oligomer. Antiviral Research 91:36-42.
817
818 Park JE, Li K, Barlan A, Fehr AR, Perlman S, McCray PB Jr, Gallagher T. 2016. Proteolytic processing
819 of Middle East respiratory syndrome coronavirus spikes expands virus tropism. Proc Natl Acad Sci U
820 S A 113:12262-7.

821 Rensi S, Altman RB, Liu T, Lo YC, McInnes G, Derry A, Keys A. Homology Modeling of TMPRSS2
822 Yields Candidate Drugs That May Inhibit Entry of SARS-CoV-2 into Human.
823 https://chemrxiv.org/articles/Homolog (preprint submitted on 20.03.2020)

824 Rockwell NC, Krysan DJ, Komiyama T, Fuller RS. 2002. Precursor processing by kex2/furin
825 proteases. Chem Rev 102:4525-48. Review.

826 Sakai K, Ami Y, Tahara M, Kubota T, Anraku M, Abe M, Nakajima N, Sekizuka T, Shirato K, Suzaki Y,
827 Ainai A, Nakatsu Y, Kanou K, Nakamura K, Suzuki T, Komase K, Nobusawa E, Maenaka K, Kuroda

M, Hasegawa H, Kawaoka Y, Tashiro M, Takeda M. 2014. The host protease TMPRSS2 plays a major role in in vivo replication of emerging H7N9 and seasonal influenza viruses. J Virol 88:5608-16.

Sarac MS, Cameron A, Lindberg I. 2002. The furin inhibitor hexa-D-arginine blocks the activation of Pseudomonas aeruginosa exotoxin A in vivo. Infect Immun 70:7136-9.

Sarac MS, Peinado JR, Leppla SH, Lindberg I. 2004. Protection against anthrax toxemia by hexa-D-arginine in vitro and in vivo. Infect Immun 72:602-5.

Shirato K, Kanou K, Kawase M, Matsuyama S. 2016. Clinical Isolates of Human Coronavirus 229E Bypass the Endosome for Cell Entry. J Virol 91:pii: e01387-16.

Shirato K, Kawase M, Matsuyama S. 2013. Middle East respiratory syndrome coronavirus infection mediated by the transmembrane serine protease TMPRSS2. J Virol 87:12552-61.

Shirato K, Kawase M, Matsuyama S. 2018. Wild-type human coronaviruses prefer cell-surface TMPRSS2 to endosomal cathepsins for cell entry. Virology 517:9-15.

Simmons G, Gosalia DN, Rennekamp AJ, Reeves JD, Diamond SL, Bates P. 2005. Inhibitors of cathepsin L prevent severe acute respiratory syndrome coronavirus entry. Proc Natl Acad Sci U S A. 102:11876-81.

Singh S, Khaytin I, Botsko S, Crossley G, Plank DK, Lefievre Y, Giuffrida F. 2002. Pennington, M. W. Addition of o-aminobenzoic acid during Fmoc solid phase synthesis of a fluorogenic substrate containing 3-nitrotyrosine. Letters in Peptide Science 9:221-5.

Stein DA. 2008. Inhibition of RNA virus infections with peptide-conjugated morpholino oligomers. Curr Pharm Des 14:2619-34.

Steinmetzer T, and Hardes, K. 2018. The Antiviral Potential of host protease inhibitors. In: Böttcher-Friebertshäuser E., Garten W., Klenk H. (eds) Activation of Viruses by Host Proteases. Springer, Cham, p.279-325. Review.

Steinmetzer T, Pilgram O, Wenzel BM, Wiedemeyer SJA. 2020. Fibrinolysis Inhibitors: Potential Drugs for the Treatment and Prevention of Bleeding. J Med Chem 63:1445-72.

Tanaka N, Tsuchiya R, Ishii K. 1979. Comparative clinical study of FOY and Trasylol in acute pancreatitis. Adv Exp Med Biol 120B:367-78.

Tarnow C, Engels G, Arendt A, Schwalm F, Sediri H, Preuss A, Nelson PS, Garten W, Klenk HD, Gabriel G, Böttcher-Friebertshäuser E. 2014. TMPRSS2 is a host factor that is essential for pneumotropism and pathogenicity of H7N9 influenza A virus in mice. J Virol 88:4744-51.

Van Lam van T, Ivanova T, Hardes K, Heindl MR, Morty RE, Böttcher-Friebertshäuser E, Lindberg I, Than ME, Dahms SO, Steinmetzer T. 2019. Design, Synthesis, and Characterization of Macrocyclic Inhibitors of the Proprotein Convertase Furin. ChemMedChem 14:673-85.

Walls AC, Park YJ, Tortorici MA, Wall A, McGuire AT, Veesler D. 2020. Structure, Function, and Antigenicity of the SARS-CoV-2 Spike Glycoprotein. Cell. pii: S0092-8674(20)30262-2.

Walls AC, Tortorici MA, Bosch BJ, Frenz B, Rottier PJM, DiMaio F, Rey FA, Veesler D. 2016. Cryo-electron microscopy structure of a coronavirus spike glycoprotein trimer. Nature 531:114-7.

Watanabe R, Matsuyama S, Shirato K, Maejima M, Fukushi S, Morikawa S, Taguchi F. 2008. Entry from the cell surface of severe acute respiratory syndrome coronavirus with cleaved S protein as revealed by pseudotype virus bearing cleaved S protein. J Virol 82:11985-91.

Zhirnov OP, Klenk HD, Wright PF. 2011. Aprotinin and similar protease inhibitors as drugs against influenza. Antiviral Res 92:27-36.

Zhou Y, Vedantham P, Lu K, Agudelo J, Carrion R Jr, Nunneley JW, Barnard D, Pöhlmann S, McKerrow JH, Renslo AR, Simmons G. 2015. Protease inhibitors targeting coronavirus and filovirus entry. Antiviral Res 116:76-84.

Figure 1

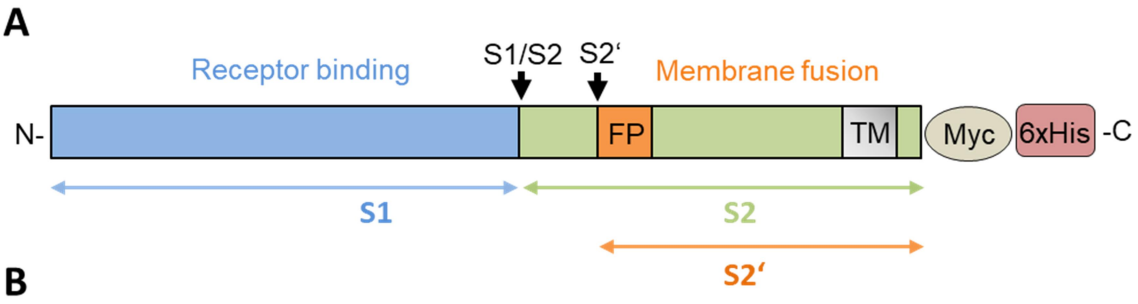

B

Virus	S1/S2 site	S2‘ site	GenBank sequence
SARS-CoV-2	TNSP**RR**A**R**↓SVA	PSKPSK**R**↓SFIEDL	YP_009724390
SARS-CoV	S----LL**R**↓STS	PLKPTK**R**↓SFIEDL	AAP13441.1
MERS-CoV	TLTP**R**SV**R**↓SVP	TGS**R**SA**R**↓SAIEDL	QFQ59587.1
HCoV-OC43	SKT**RR**S**RR**↓AIT	CSKASS**R**↓SAIEDL	AMK59677.1
HCoV-229E	SIIAVQP**R**↓NVS	GSRVAG**R**↓SAIEDI	APT69890.1
HCoV-NL63	SLIPVRP**R**↓NSS	SSRIAG**R**↓SALEDL	AFV53148.1
HCoV-HKU1	SSS**RRKRR**↓SIS	CGS-SS**R**↓SFFEDL	AAT98580.1
IBV Beaudette	NGT**RR**F**RR**↓SIT	PSS**RRKR**↓SLIEDL	CAC39300.1

Figure 1: Cleavage of coronavirus S protein. A) Schematic representation of the SARS-CoV-2 precursor and the S1 and S2 subunits. Fusion peptide (FP), transmembrane domain (TM). The S1/S2 and S2′ cleavage sites and subunits S1, S2 and S2‘ are indicated by black and coloured arrows, respectively. For immunochemical detection recombinant S is expressed with a C-terminally fused Myc-6xHis-tag peptide in our study. **B)** Alignment of the amino acid sequences at the S1/S2 and S2‘ cleavage site of the S proteins of different human coronaviruses (HCoV) and avian infectious bronchitis virus (IBV) strain Beaudette.

Figure 2

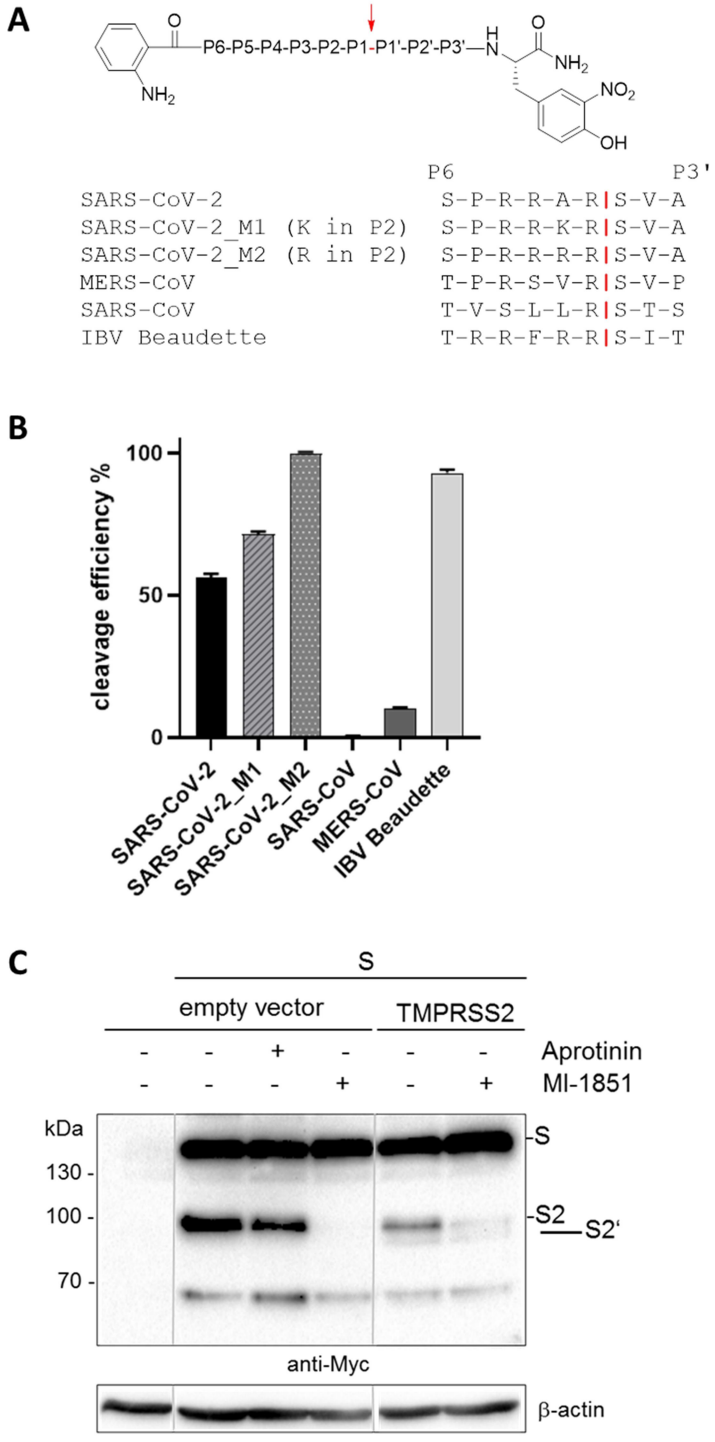

Figure 2: Cleavage of SARS-CoV-2 S by furin and TMPRSS2. A) FRET substrates of the S protein S1/S2 sites of the indicated CoVs. M1 and M2 are mutants of the SARS-CoV-2 S1/S2 site with substitution of A→K or A→R in P2 position. IBV: avian infectious bronchitis virus strain Beaudette. Cleavage by furin is indicated in red. **B)** Cleavage of the FRET substrates (20 µM) by furin (0.5 nM). Cleavage efficiency of SARS-CoV-2_M2 was set as 100 %. **C)** Cleavage of SARS-CoV-2 S by furin and TMPRSS2 in HEK293 cells. Cells were

co-transfected with pCAGGS-S-Myc-6xHis and either empty vector or pCAGGS-TMPRSS2. Cells were then incubated in the absence or presence of aprotinin or furin inhibitor MI-1851 (50 µM each) for 48 h. Cell lysates were subjected to SDS-PAGE and Western blot analysis using antibodies against the C-terminal Myc-tag. Lanes are spliced together from one immunoblot from one experiment.

Figure 3

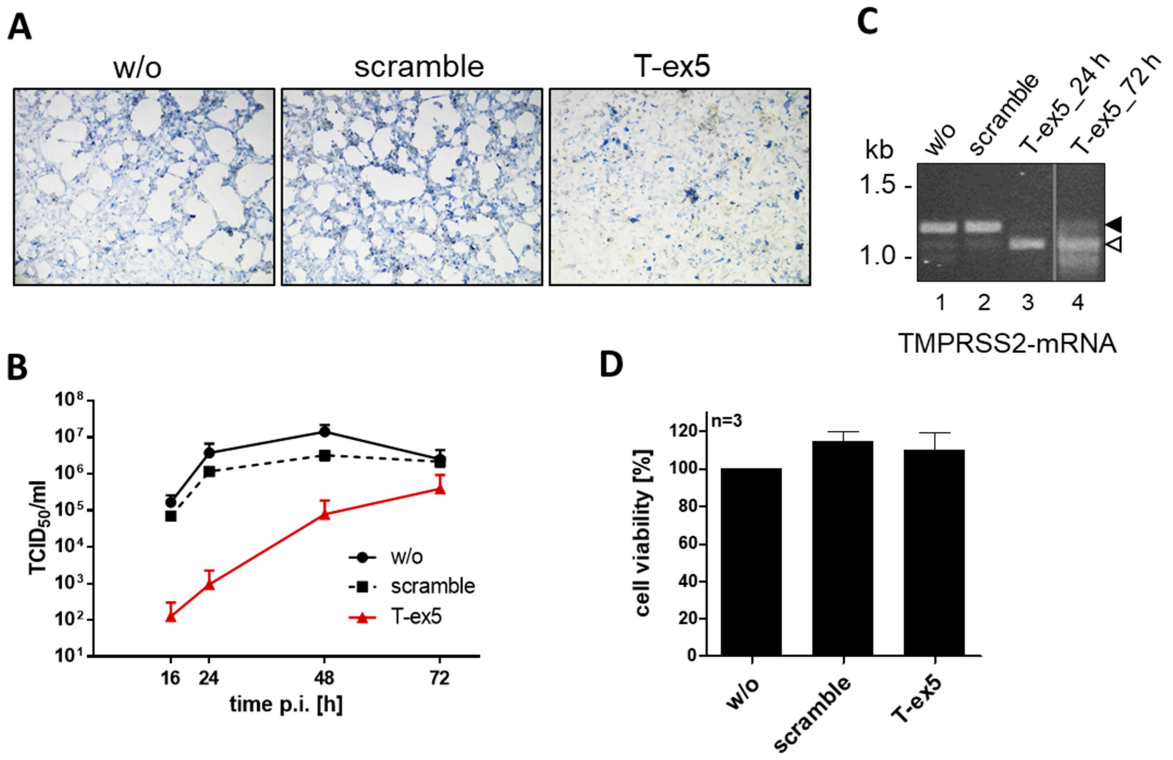

Figure 3: Knockdown of TMPRSS2 expression by PPMO T-ex5 inhibits multicycle replication of SARS-CoV-2 in Calu-3 cells. A) Multicycle replication of SARS-CoV-2 in T-ex5 treated Calu-3 cells. Cells were treated with 25 µM T-ex5 or control PPMO (scramble) for 24 h or remained untreated (w/o), then inoculated with SARS-CoV-2 at a MOI of 0.001 and further incubated in the absence of PPMO for 72 h. Cells were fixed and immunostained using a serum against SARS-CoV. **B)** Calu-3 cells were treated with PPMO for 24 h and then infected with SARS-CoV-2 for 72 h as described above. Virus titers in supernatants were determined by tissue culture infection dose 50 % ($TCID_{50}$) end-point dilution at indicated time points. Results are mean values ± standard deviations (SD) of two independent experiments (n=2). **C)** Analysis of TMPRSS2-mRNA in PPMO-treated Calu-3 cells. Cells were treated with 25 µM T-ex5, scramble PPMO or remained untreated (w/o) for 24 h (lanes 1-4). T-ex5 treated cells were inoculated with SARS-CoV-2 as described above and incubated in the absence of PPMO for 72 h (lane 4). Total RNA was isolated and analysed by RT-PCR using primers designed to amplify 1228 nt of full-length TMPRSS2-mRNA. Full-length and truncated PCR product lacking exon 5 are indicated by filled and open arrow heads, respectively. **D)** Effect of PPMO treatment on Calu-3 cell viability. Calu-3 cells were treated with scramble or T-ex5 PPMO (25 µM) for 24 h. Cell viability of untreated (w/o) cells was set as 100 %. Results are mean values ± SD (n=3).

Figure 4

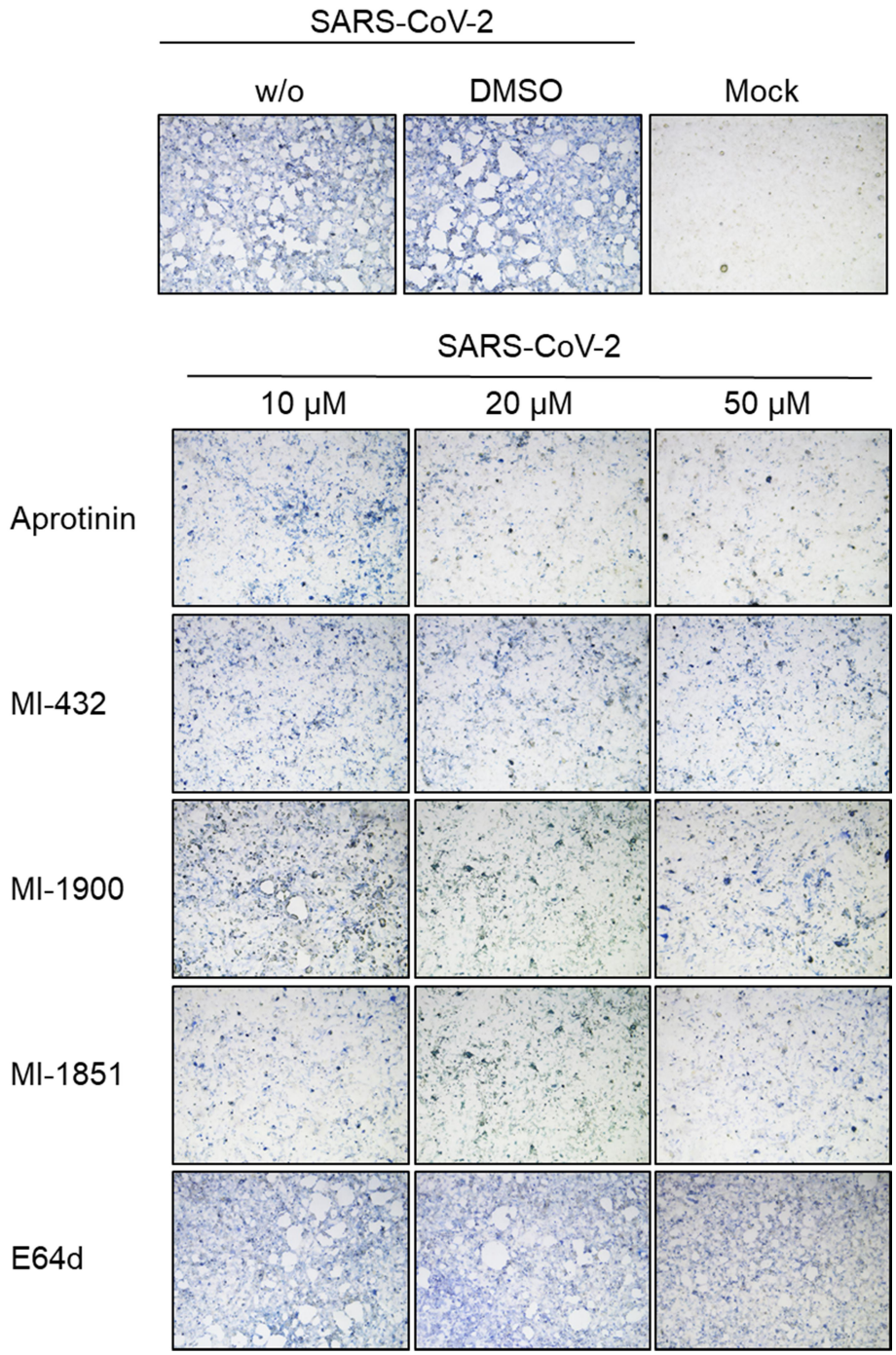

Figure 4: Inhibition of SARS-CoV-2 multiplication in human airway cells by inhibitors of furin and TMPRSS2. Calu-3 cells were inoculated with SARS-CoV-2 at a low MOI of 0.001 and then incubated in the presence of inhibitors of TMPRSS2 (aprotinin, MI-432, MI-1900), furin (MI-1851), and endosomal cathepsins (E64d), respectively, at the indicated concentrations. Cells were fixed and immunostained using a rabbit serum against 2002 SARS-CoV at 72 h post infection (p.i.). Cells infected in the absence of inhibitors (w/o), in the presence of DMSO (0.5 %) and non-infected cells (mock) were used as controls. Images are representatives of three independent experiments.

Figure 5

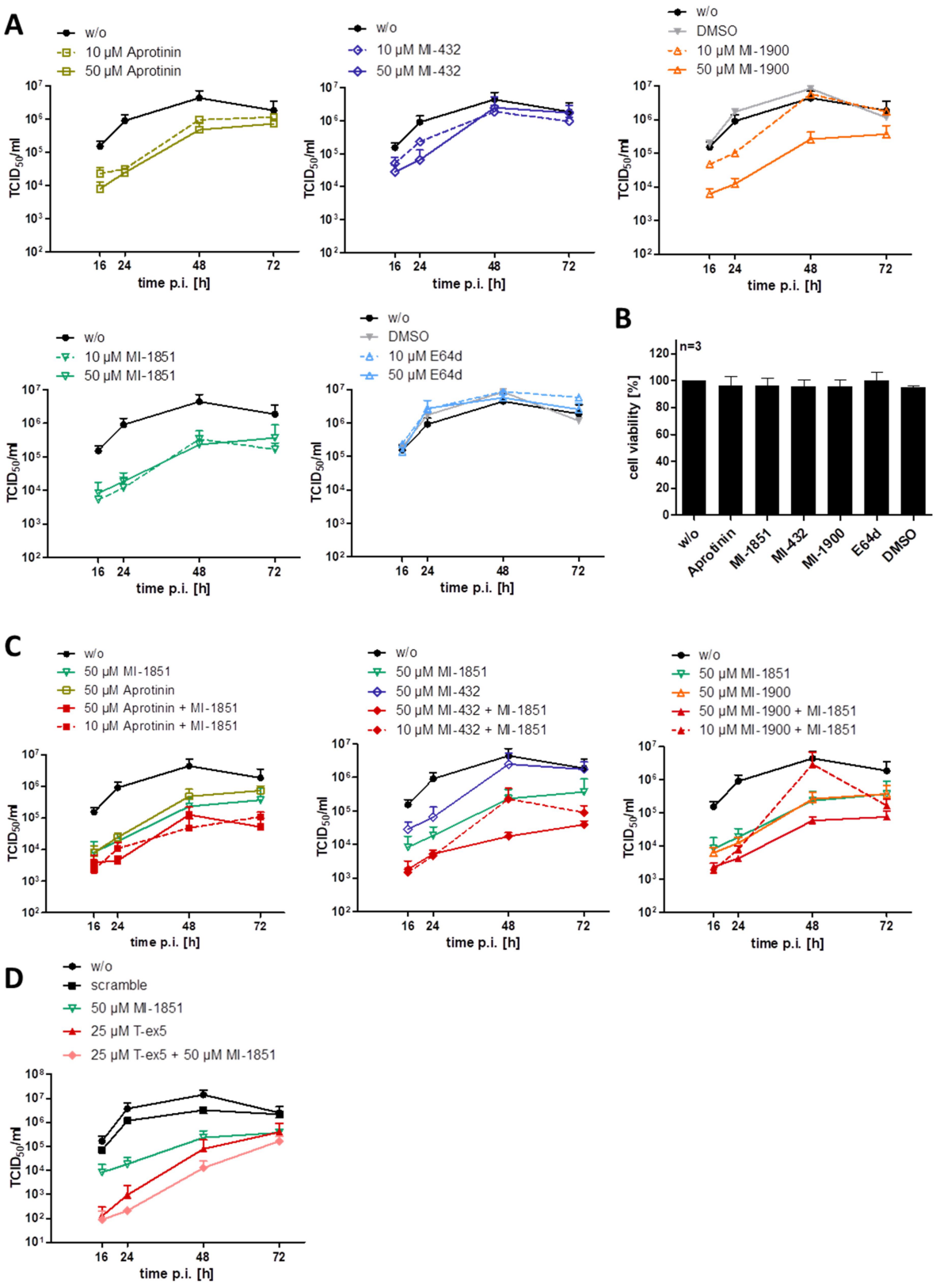

Figure 5: Inhibition of SARS-CoV-2 multicycle replication in human airway epithelial cells by inhibitors of TMPRSS2 and furin. A) Calu-3 cells were inoculated with SARS-CoV-2 at a low MOI of 0.001 and then incubated in the absence (w/o) or presence of

inhibitors of TMPRSS2 (aprotinin, MI-432, MI-1900), furin (MI-1851), and endosomal cathepsins (E64d), respectively, or DMSO (0.5 %), at the indicated concentrations. At 16, 24, 48, and 72 h p.i., supernatants were collected, and virus replication was determined by $TCID_{50}$ titration at indicated time points. Data are mean values ± SD from two to four independent experiments. **B)** Effect of inhibitor treatment on cell viability. Calu-3 cells were treated with the indicated protease inhibitor (50 µM) for 72 h. Untreated cells (w/o) and DMSO treated cells were used as controls. Cell viability of untreated cells was set as 100 %. Results are mean values ± SD (n=3). **C)** Antiviral activity of combinations of TMPRSS2 and furin inhibitors against SARS-CoV-2 in human airway epithelial cells. Calu-3 cells were inoculated with SARS-CoV-2 at a MOI of 0.001 as described above and then incubated in the presence of single protease inhibitors or inhibitor combinations at the indicated concentrations. Virus titers in supernatants were determined by $TCID_{50}$ at 16, 24, 48 and 72 h p.i.. Data are mean values ± SD of two to three independent experiments. **D)** Calu-3 cells were treated with PPMO for 24 h, then infected with SARS-CoV-2 as described above and incubated in the absence of PPMO (w/o, scramble and T-ex5) and with or without 10 µM of furin inhibitor treatment (MI-1851) for 72 h. At 16, 24, 48, and 72 h p.i., supernatants were collected, and viral titers were determined by $TCID_{50}$ at indicated time points. Data are mean values ± SD (n=2).

Figure 6

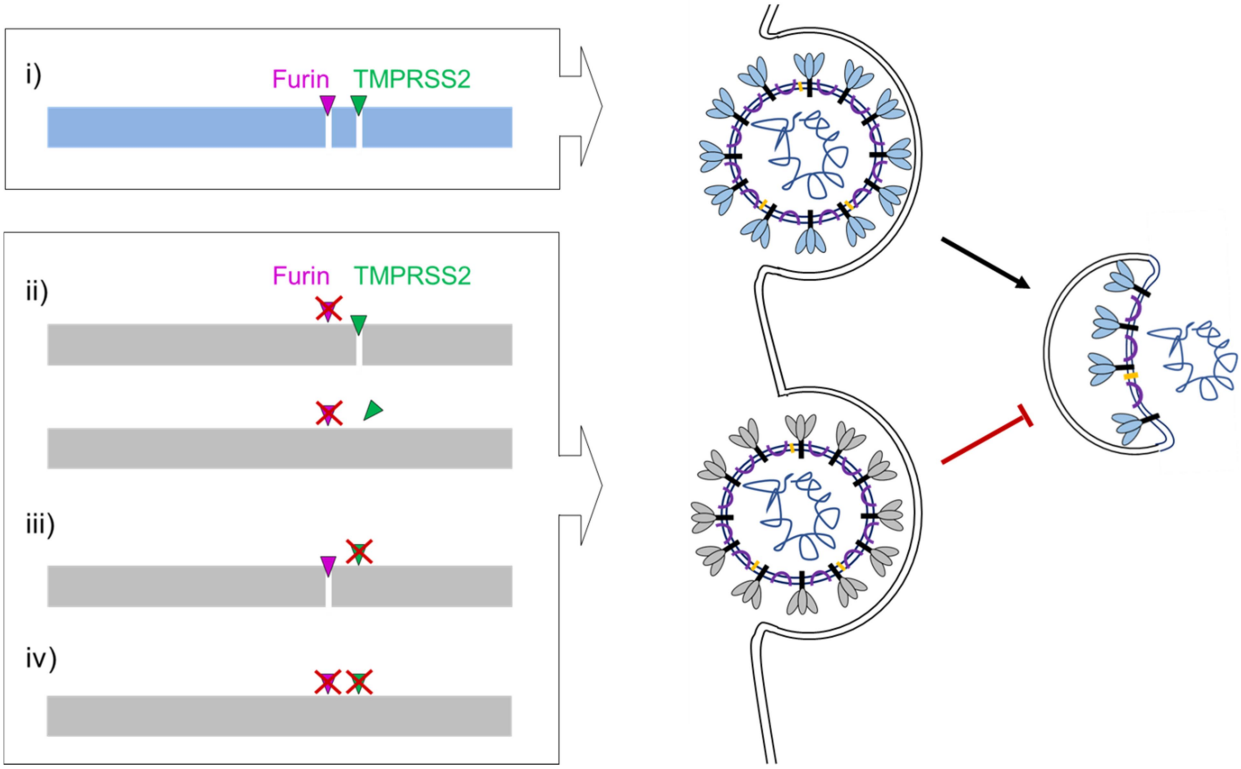

Figure 6: Proposed processing of SARS-CoV-2 spike protein S by TMPRSS2 and furin. **i)** S must be cleaved at two sites, S1/S2 and S2‘, to trigger fusion of viral and cellular membranes during virus entry in order to release the virus genome into the host cell. CoV S cleavage is believed to occur sequentially, with cleavage at the S1/S2 site occurring first and subsequent cleavage at the S2′ site. Furin processes the S1/S2 site, whereas TMPRSS2 cleaves at the S2‘ site, and both proteases cannot compensate each other. Inhibition of either furin (ii) or TMPRSS2 (iii) or simultaneous inhibition of both proteases (iv) renders the S protein fusion-inactive and prevents virus entry. Inhibition of TMPRSS2 prevents exposure of the fusion peptide at the N-terminus of the S2‘ subunit (iii and iv). Inhibition of furin cleavage at the S1/S2 site may directly interfere with virus entry and membrane fusion by steric blockage of conformational changes (ii, upper scheme) or may prevent exposure of the S2‘ site to TMPRSS2 (ii, lower scheme). Fusion-competent S is indicated in blue, fusion-incompetent S in grey.

Figure S1

MI-432

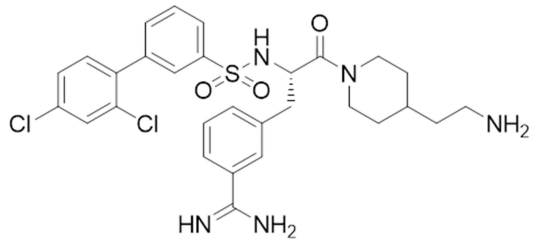

MI-1900

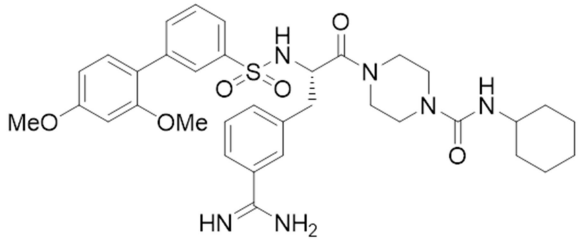

MI-1851

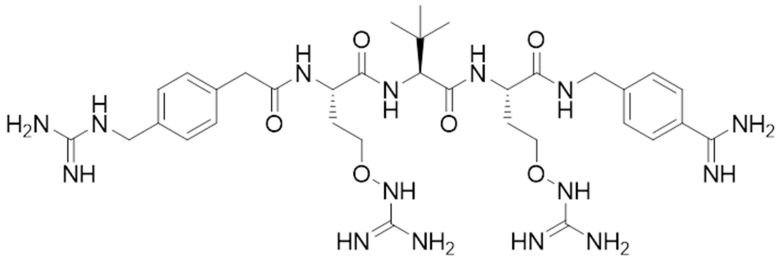

Aprotinin

RPDFCLEPPYTGPCKARIIRYFYNAKAGLCQTFVYGGCRAKRNNFKSAEDCMRTCGGA

Figure S1: Structural formulas of peptide mimetic inhibitors MI-432, MI-1900 and MI-1851 and the linear amino acid sequence of bovine aprotinin (Kassell et al., 1965).

Figure S2

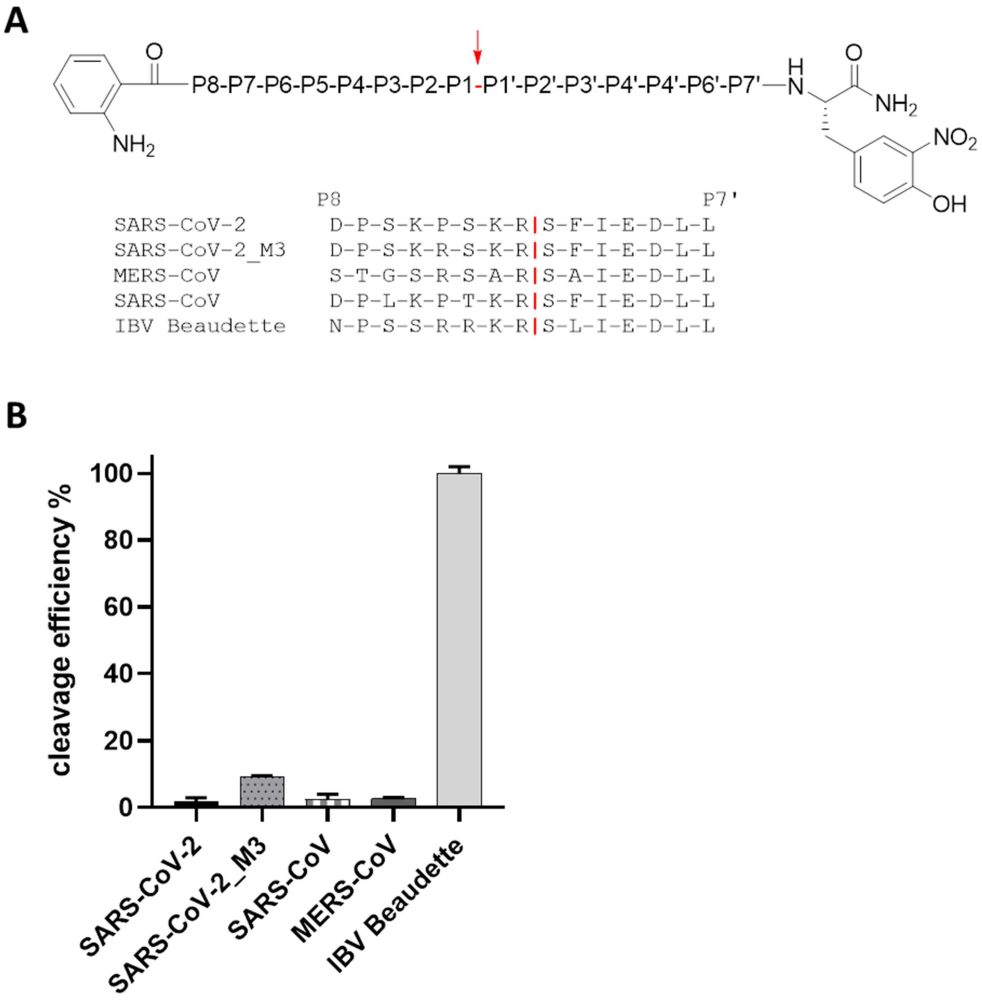

Figure S2: Cleavage analysis of SARS-CoV-2 S2‘ site by furin. **A)** FRET substrates of the S protein S2‘ sites of the indicated CoVs. M3 is a mutant of the SARS-CoV-2 S2‘ site with substitution of P→R in P4 position. IBV: avian infectious bronchitis virus strain Beaudette. Cleavage by furin is indicated in red. **B)** Cleavage of the FRET substrates (20 µM) by furin (0.5 nM). Cleavage efficiency of IBV Beaudette was set as 100%.